Tetrahedron 66 (2010) 6205–6211

Contents lists available at ScienceDirect

Tetrahedron

journal homepage: www.elsevier.com/locate/tet

# Theoretical study on structural and mechanistic aspects of synthesis of a 3-aminopyrazole derivative

Svetlana Marković [a], Milan D. Joksović [a,*], Petra Bombicz [b], Vukadin M. Leovac [c], Violeta Marković [a], Ljubinka Joksović [a]

[a] Faculty of Sciences, University of Kragujevac, R. Domanovića 12, 34000 Kragujevac, Serbia
[b] Institute of Structural Chemistry, Chemical Research Center, Hungarian Academy of Sciences, PO Box 17, H-1525 Budapest, Hungary
[c] Faculty of Sciences, University of Novi Sad, Trg D. Obradovića 3, 21000 Novi Sad, Serbia

ARTICLE INFO

*Article history:*
Received 2 March 2010
Received in revised form 6 May 2010
Accepted 24 May 2010
Available online 4 June 2010

*Keywords:*
Crystal structure
Reaction mechanism
Keto-imine tautomer
DFT
3-Aminopyrazole

ABSTRACT

The structure of 5-hydroxy-3,5-dimethyl-1-*S*-methylisothiocarbamoyl-2-pyrazolinium iodide (HDMCPI), a cyclic intermediate for a 3-aminopyrazole derivative, was determined by means of X-ray analysis and spectroscopic techniques. In a treatment of HDMCPI in alkaline aqueous solution, 4-acetyl-3(5)-amino-5(3)-methylpyrazole (AAMP) was unexpectedly yielded. The reaction of HDMCPI was monitored by $^{1}H$ and $^{13}C$ NMR spectroscopy. It was shown that keto-imine tautomer appears as the only tautomeric form. Density functional theory explained the spontaneous formation of keto-imine tautomer, whose existence is the main condition for generating a carbanion in alkaline medium. The carbanion further undergoes cyclization and elimination of MeSH, thus yielding AAMP. In the reaction of acetylacetone with thiosemicarbazide instead of *S*-methylisothiosemicarbazide, there were no traces of AAMP. This result can be attributed to the absence of keto-imine form in the tautomeric equilibrium, which would provide the formation of a carbanion for a nucleophilic attack and further cyclization.



## 1. Introduction

The chemistry of 3-aminopyrazole has remained largely underdeveloped until the discovery of its derivatives as antitumor agents with their great therapeutic potential against various proliferative disorders in the role of chemical inhibitors of cyclin-dependent kinases (CDKs), a family of enzymes involved in controlling normal cell proliferation.[1–4] The frequent deregulation of cell cycle progression in cancer has intensified search for kinase inhibitors with high affinity and specificity over the past several years.[5–7] PHA-739358, a small molecule of 3-aminopyrazole derivative with strong activity against Aurora kinases and cross-reactivities with some receptor tyrosine kinases, exhibits significant antitumor activity in a wide range of cancers and shows a favorable pharmacokinetic and safety profile.[8] Recently, a series of 3-aminopyrazole based Aurora kinase inhibitors with a pyrimidine scaffold led to a class of very potent inhibitors of cellular proliferation in treatment of chronic myelogenous leukemia or Philadelphia chromosome-positive acute lymphoblastic leukemia.[9] Very recently, a selective 3-aminopyrazole MK2 kinase inhibitors were discovered and profiled to show potent inhibition MK2 activity and reasonable cellular activity.[10]

Although the synthesis of 4-acetyl-3(5)-amino-5(3)-methylpyrazole (AAMP) has been reported about two decades ago,[11] the recent discoveries in the field of 3-aminopyrazole derivatives and their pharmacological and medicinal importance prompted us to shed much more light on the mechanism of formation of AAMP, starting from relatively simple precursors. In the present study we have focused our attention on theoretical and mechanistical aspects of the synthesis of this 3-aminopyrazole derivative, as a high versatile precursor for preparation of a number of potential kinase inhibitors bearing in mind the great possibilities of transformation of acetyl group linked to 3-aminopyrazole scaffold.

## 2. Results and discussion

### 2.1. The crystal structure of 5-hydroxy-3,5-dimethyl-1-*S*-methylisothiocarbamoyl-2-pyrazolinium iodide (HDMCPI)

The crystal data, details of structure determination and refinement of HDMCPI are given in the Supplementary data. The iodide anion is hydrogen bonded to the organic moiety by the O5–H5···I1 and N7–H7A···I1 interactions (Fig. 1a, Table 1). The packing coefficient is 65.7%, there is no residual solvent accessible void. The basic building unit of the crystal is a dimer organized by the symmetry centre (Fig. 1b, Table 1). H7B is a bifurcated hydrogen

* Corresponding author. E-mail address: mjoksovic@kg.ac.rs (M.D. Joksović).

0040-4020/$ – see front matter © 2010 Elsevier Ltd. All rights reserved.
doi:10.1016/j.tet.2010.05.093

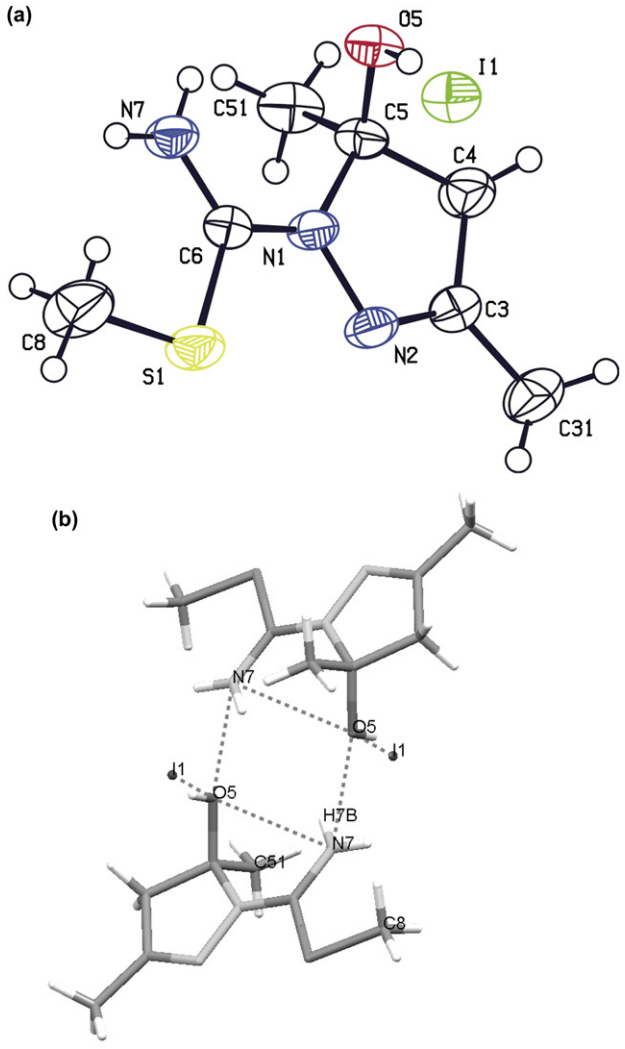


**Figure 1.** ORTEP representation[13] of HDMCPI at 50% probability level, heteroatoms are shaded. (b)The dimer formed in the structure of HDMCPI and the connected iodide organized by the symmetry centre.[14]

**Table 1**
Intermolecular interactions in the crystal structure of HDMCPI

| D–H···A | Type | D–H [Å] | H···A [Å] | D···A [Å] | D–H···A [°] | Symmetry operation |
|---|---|---|---|---|---|---|
| N7–H7B···O5 | Intra | 0.86 | 2.37 | 2.903 (3) | 121 | |
| O5–H5···I1 | In asym unit | 0.82 | 2.62 | 3.399 (3) | 159 | |
| N7–H7A···I1 | Inter | 0.86 | 2.83 | 3.612 (3) | 153 | $x, 1+y, z$ |
| N7–H7B···O5 | Inter | 0.86 | 2.23 | 3.003 (3) | 149 | $1-x, 1-y, 1-z$ |
| C51–H51A···I1 | Inter | 0.96 | 3.05 | 3.993 (4) | 167 | $-1/2+x, 1/2-y, -1/2+z$ |
| C8–H8A···I1 | Inter | 0.96 | 3.05 | 3.886 (5) | 146 | $1/2-x, 1/2+y, 3/2-z$ |

atom, taking part in both intramolecular and intermolecular hydrogen bonds to O5 oxygen atoms. The graph set description[12] of the ring formed by the hydrogen bonds is $R^2_2(6)$. The neighboring dimers are kept together by weak C–H···O interactions. A herring bone arrangement can be observed from the crystallographic *a* direction in the packing diagram (Supplementary data).

The structure of HDMCPI was reproduced using density functional theory (DFT), in order to test the suitability of the applied computational method. The obtained bond lengths, bond angles, and dihedral angles are provided in Tables S5–S7 of Supplementary data. The average relative errors for bond angles and dihedral angles amount 0.89 and 0.45%, respectively. The lengths of the bonds including hydrogen are overestimated, whereas the average relative error for bond lengths among heavy atoms equals 0.99%. Such agreement between the experimental and computed structure of HDMCPI confirms the applicability of the used DFT method.

## 2.2. Mechanistic studies

The synthesis of 4-acetyl-3(5)-amino-5(3)-methylpyrazole (AAMP) starting from acetylacetone and *S*-methylisothiosemicarbazide hydrogen iodide has been already described,[11] but the intermediate was incorrectly presented, only on the basis of elemental analysis, as acetylacetone mono-*S*-methylisothiosemicarbazone. Now, we have obtained single crystals suitable for X-ray analysis, and using spectroscopic methods completely characterized this compound as the cyclic compound 5-hydroxy-3,5-dimethyl-1-*S*-methylisothiocarbamoyl-2-pyrazolinium iodide (HDMCPI) (Scheme 1).

The values of bond lengths between the carbon and two nitrogens of *S*-methylisothiocarbamoyl group indicate delocalization of positive charge through all three atoms in the solid state. In addition, the natural bond orbital (NBO) analysis of HDMCPI shows strong donation of density from the p orbitals on N7 and S to the $\pi^*$ antibonding N1–C6 orbital, and from the $sp^{0.45}$ orbital on S to the $\sigma^*$ antibonding C6–N7 orbital, thus confirming the delocalization in the *S*-methylisothiocarbamoyl group. However, in DMSO-$d_6$ solution, the $^1$H NMR spectra, except for two singlets ($C_3$–Me and $C_5$–Me) and one AB system for the pyrazoline ring protons, shows two singlets for S–Me protons, as well as two groups of signals at lower field. The first, two broad singlets, one bigger at 7.73 ppm and a smaller one at 7.52 ppm of the total relative intensity 1, can be attributed to two kinds of hydroxyl protons. The second set of three broad peaks, one bigger at 8.80 ppm and two smaller at 8.96 and 9.42 ppm of the total relative intensity 2 can be assigned to the nitrogen protons. Three smaller peaks were in an intensity ratio of 1:1:1 while bigger signals at 8.80 ppm and 7.73 ppm were in an intensity ratio 2:1, respectively. These facts suggest that not only one form of HDMCPI was present in the DMSO-$d_6$ solution. In order to consider an explanation of this $^1$H NMR complexity, we must take into an account the existence of other distinct tautomers with possibly different NMR spectra whose concentration will vary with selected deuterated solvent. For example, a proton could be moved from the exocyclic nitrogen onto ring nitrogen atom giving a structure with three chemically nonequivalent protons with the same intensities (Scheme 2).

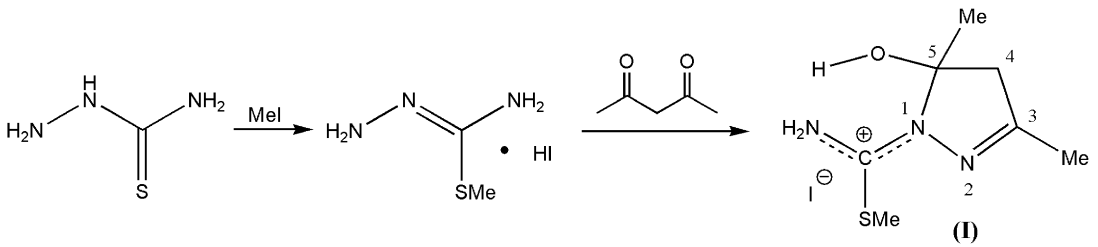


**Scheme 1.** Synthesis of HDMCPI (*I*).

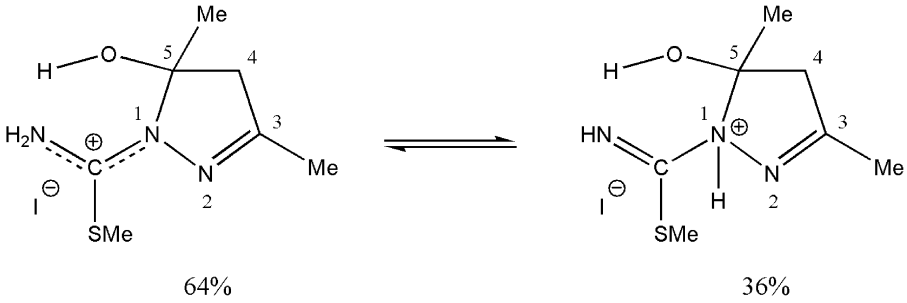


**Scheme 2.** Two possible tautomeric forms of HDMCPI in DMSO-$d_6$ solution (the ratio of tautomers is determined by integration of $^1$H NMR signals).

Addition of $D_2O$ to the DMSO-$d_6$ solution caused the collapse of the AB system to a singlet and disappearance of the N–H and the O–H protons because of fast exchange of these protons with $D_2O$. Simultaneously, one singlet attributable to the S–Me protons was observed instead of two singlets in DMSO-$d_6$ solution. Finally, in pure $D_2O$ solution all signals appeared only as singlets.

Dissolving HDMCPI in an alkaline aqueous solution (pH>13) unexpectedly affords AAMP after about 15 h of standing at room temperature, in the forms of white needle-like crystals. In order to slow this reaction for $^1$H NMR monitoring, we dissolved HDMCPI in $D_2O$ and adjusted pD to 9.5 by careful addition of NaOD. Bearing in mind that thiosemicarbazones of 1,3-dicarbonylic compounds are complex multitautomeric systems, we could expect an equilibrium mixture of several open-chain tautomeric forms in the solution, including the cyclic one with predominance of keto-enamine form.[15,16] It has been known that the tautomeric equilibria are very sensitive to pH and the polarity of the solvent.[17] However, after analyzing the $^1$H and $^{13}$C NMR spectra at pD=9.5 we have observed surprisingly that this compound is present in $D_2O$ only in the form of keto-imine tautomer A (Scheme 3). The presence of the keto-imine tautomer A in solution is unambiguously indicated by the $^{13}$C NMR spectrum, in which a resonance signal at the high $\delta$ value of 214.3 ppm is in the range characteristic of aliphatic ketones, not that of keto-enamines or enol-imine forms.[18] Further evidences, confirming the structure of A result from a systematic pattern of isomer peaks of the methyl group typical for *S*-alkylated thiosemicarbazones due to cis/trans isomerism from the C=N double bond.[19] The $^{13}$C NMR spectrum also has complex broad signal at 50.1 ppm corresponding to the carbon between carbonyl and imino group. Other details of the $^1$H and $^{13}$C NMR spectra agree with keto-imine tautomeric form.

This finding motivated us to investigate the mechanism of the formation of A from the HDMCP cation using DFT calculations. If Gibbs free energy ($G^{298}$) is taken as a measure of tautomer stability, it turns out that A is less stable than B and C by 18.1 and 2.8 kJ/mol, respectively. The $G^{298}$ values are in agreement with a simple chemical reasoning, based on the fact that B and C are stabilized with strong hydrogen bonds. On the basis of these facts, the presence of tautomer A is not expected as the only form in the tautomeric equilibrium.

To explain this unexpected experimental finding, we examined possible interactions between the HDMCP cation and hydroxide anion. All examined pathways are here presented. Our investigation did not reveal any transition state for a reaction pathway between the HDMCP cation and hydroxide anion. On the other hand, our attempts to optimize a structure consisting of the HDMCP cation and hydroxide anion resulted in a spontaneous transfer of a proton (i.e., without activation barrier) from the hydroxyl group of the HDMCP cation to the $OH^-$ anion. This rearrangement includes a ring opening, and formation of the structure D (Fig. 2), with the stabilization of the system of 143.2 kJ/mol. It is worth pointing out that structure D is actually a hydrated tautomeric form A. The tautomer A can be transformed into B via transition state TS1, requiring an activation barrier of 185.0 kJ/mol, whereas B can rearrange into C via transition state TS2, requiring an activation energy of 14.8 kJ/mol (Fig. 2). A reaction path for a transformation of A into C was not revealed. One can conclude, on the basis of the presented activation energies, that the only pathway for transformation of the HDMCP cation in alkaline medium is the formation of the tautomer A. In this way the presence of A as the only form in tautomeric equilibrium is explained.

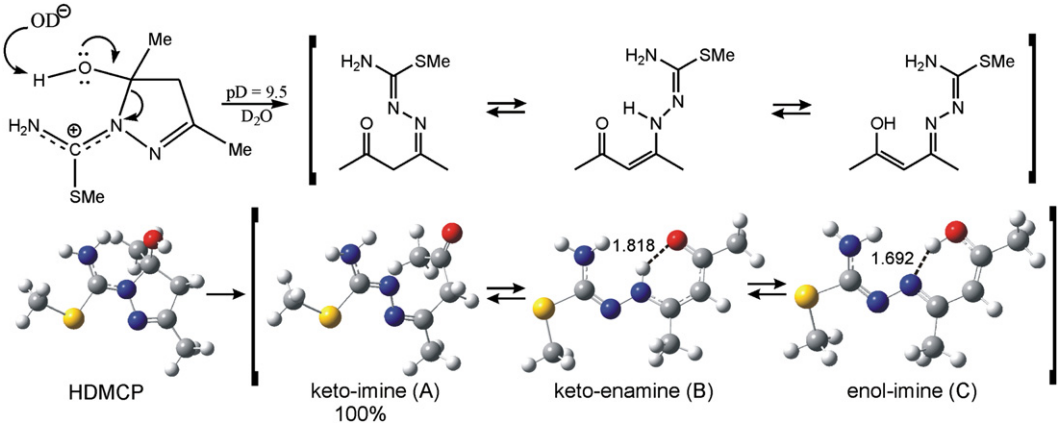


**Scheme 3.** Tautomeric forms of 5-hydroxy-3,5-dimethyl-1-*S*-methylisothiocarbamoyl-2-pyrazolinium cation (HDMCP).

Our investigation shows that in alkaline medium tautomer A can undergo pathways that lead to the formation of carbanions. Namely, the acidic hydrogens of A can delocalize the charge of the hydroxide anion, forming structure E in Scheme 4. Three reaction pathways were revealed for the transformation of E, where the carbanions CA1, CA2, and CA3 were formed. The activation energies for the formation of CA1, CA2, and CA3 amount 4.9, 8.8, and 31.3 kJ/mol, respectively. As expected, $G^{298}$ of CA2 is lower than those of CA1 and CA3 by 27.1

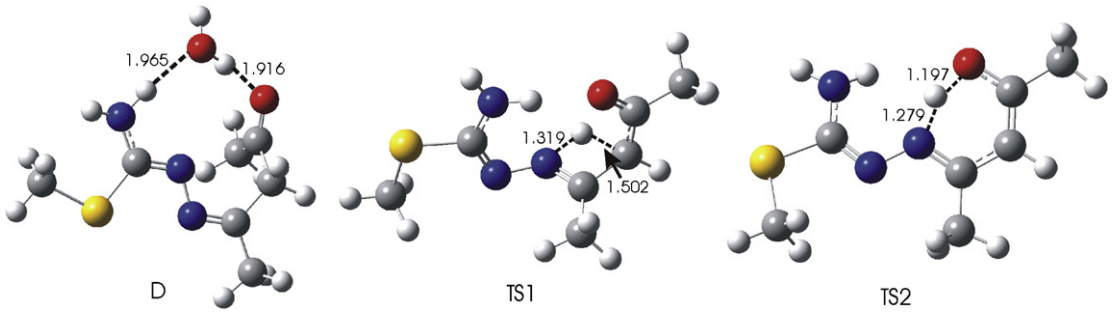


**Figure 2.** Optimized structures of hydrated tautomer A (D), and transition states TS1 and TS2.

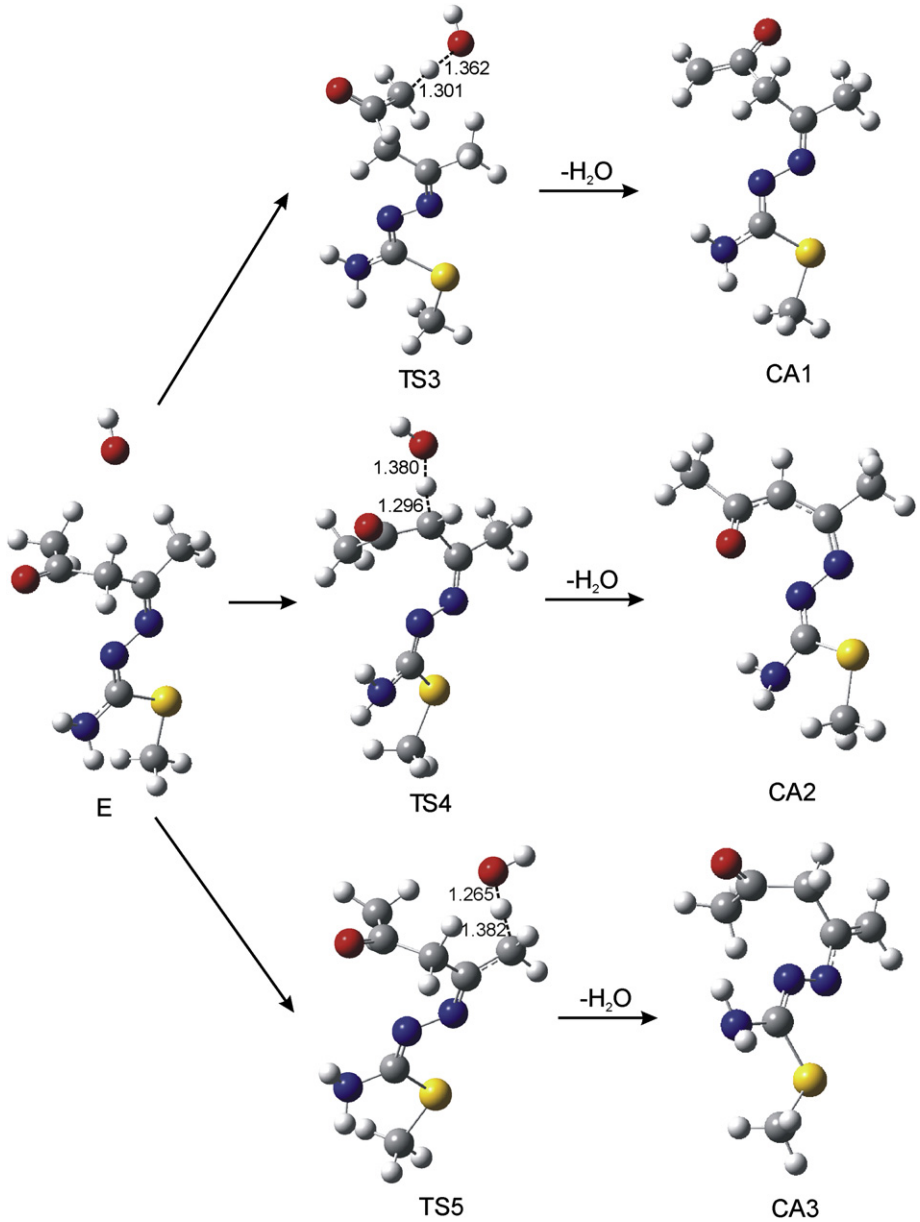


**Scheme 4.** Mechanism of formation of carbanions CA1, CA2, and CA3, via transition states TS3, TS4, and TS5, respectively.

and 61.3 kJ/mol, respectively. Taking into account low activation energy and pronounced stability of CA2, we assume that the main reaction path for the transformation of A is the formation of CA2. Thus, the existence of tautomeric form A is the main condition for generating the carbanion CA2 in alkaline medium.

The natural resonance analysis of CA2 revealed the possibility of its resonance stabilization. The major resonance structures of CA2 are presented in Scheme 5. The numbers below the resonance structures denote the resonance weights in the equilibrium geometry of CA2. It is obvious that the resonance structure with the 25.3%

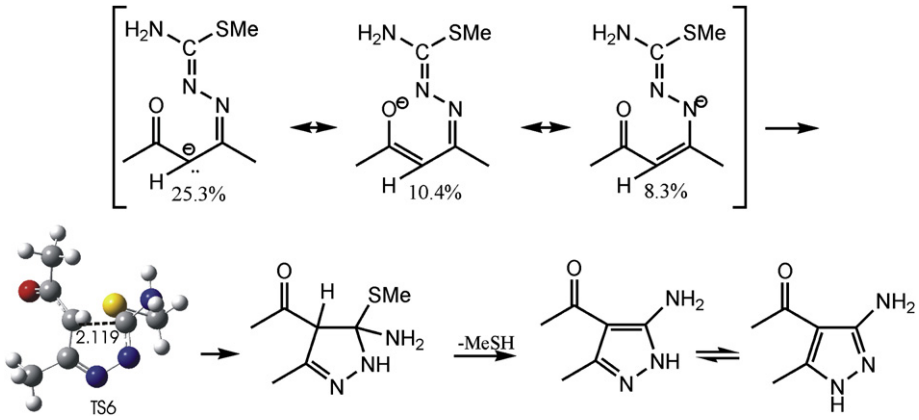


**Scheme 5.** Possible mechanism of formation of AAMP.

resonance weight dominates in the resonance hybrid, thus providing the conditions for nucleophilic attack and further cyclization.

The carbanion structure (that with the highest resonance weight) gives the possibility for intramolecular nucleophilic attack on the very electrophilic carbon of the C=N group, leading to the formation of the corresponding cyclic pyrazoline compound. This step of the reaction proceeds via transition state TS6 (Scheme 5), and requires activation barrier of 115.7 kJ/mol. The elimination of MeSH takes place easily in an alkaline medium, followed by an unpleasant mercaptane odor, yielding the tautomeric equilibrium of corresponding pyrazoles.[20]

In order to confirm our hypothesis about the crutial role of keto-imine tautomer, we repeated the same experiment with carbon atom of the conjugated carbonyl group at 183.04 ppm. These data agree with the spectra of many enamines.[18,21] It is evident that the absence of the keto-imine form (F) in the tautomeric equilibrium does not allow any possibility of the formation of a carbanion for a nucleophilic attack and further cyclization. Also, we detected 3,5-dimethylpyrazole-1-thiocarboxamide as a consequence of the dehydration of pyrazolinol compound. The structure of this compound was confirmed by comparison with authentic sample. It is notable that cyclic pyrazolinol (Scheme 6) is a very unstable compound even in the solid state. Its decomposition begins after several hours and all material was transformed into 3,5-dimethylpyrazole-1-thiocarboxamide after two weeks of standing.

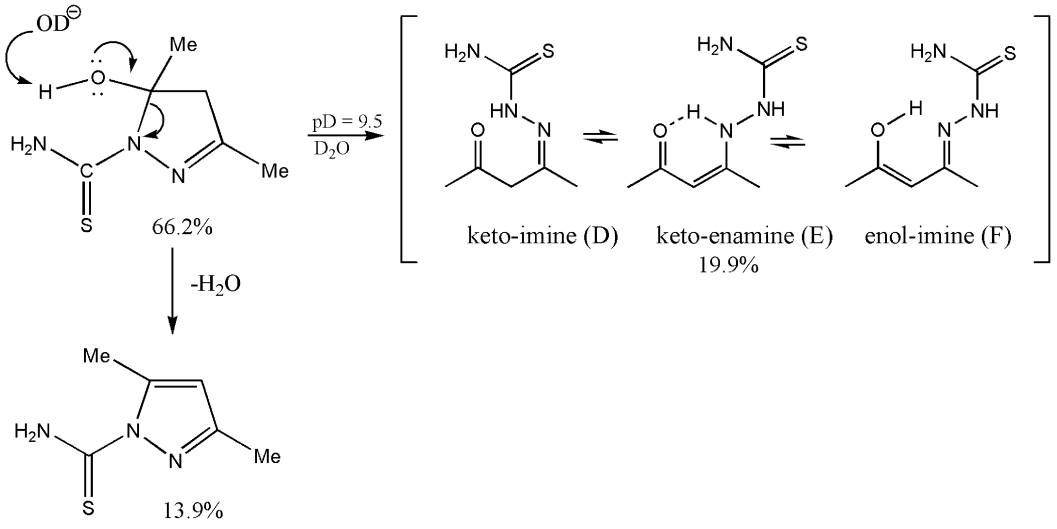


**Scheme 6.** Tautomeric forms of 5-hydroxy-3,5-dimethyl-1-thiocarbamoyl-2-pyrazoline. The ratio of tautomer (E), 3,5-dimethylpyrazole-1-thiocarboxamide and starting pyrazoline compound was determined by integration of $^{1}$H NMR signals of the methyl groups.

thiosemicarbazide instead of *S*-methylisothiosemicarbazide in the reaction with acetylacetone preparing its cyclic analogue 5-hydroxy-3,5-dimethyl-1-thiocarbamoyl-2-pyrazoline (Scheme 6) according to the known procedure.[15]

After 15 h of standing in highly alkaline solution (pH>13) there were no traces of AAMP. Then we adjusted pD at 9.5, and the almost quantitatively formed white solid was analyzed by $^{1}$H and $^{13}$C NMR in the same conditions for comparison with S-methylated derivative. We established that the main form in the state of the equilibrium in DMSO-$d_6$ solution is the starting cyclic compound (Scheme 6) The keto-enamine form (G) in the NMR spectrum of the mixture was presented as vinyl proton signal at 6.48 ppm as well as the α-carbon of the vinyl group at 84.98 and a signal for the

## 3. Conclusion

The agreement between experimentally obtained and calculated bond distances, bond angles, and torsion angles of 5-hydroxy-3,5-dimethyl-1-*S*-methylisothiocarbamoyl-2-pyrazolinium iodide (HDMCPI) is very good, confirming that the selected computational method is suitable for investigating the reactions of HDMCPI. In this work, the transformation of 5-hydroxy-3,5-dimethyl-1-*S*-methylisothiocarbamoyl-2-pyrazolinium cation (HDMCP) in alkaline aqueous solution was investigated using experimental and computational methods.

It was shown that the reaction between the HDMCP cation and hydroxyde anion proceeds smoothly, without activation barrier,

and with significant stabilization of the system. In this way the hydrated keto-imine tautomer A is formed, at 100% yield. The activation energy for the isomerization of A into keto-enamine tautomer B is significantly higher in comparison to the formation of carbanion CA2 in alkaline medium. CA2 undergoes further cyclization and elimination of MeSH, thus yielding 4-acetyl-3(5)-amino-5(3)-methylpyrazole (AAMP).

The absence of AAMP as a product of the reaction between acetylacetone with thiosemicarbazide instead of *S*-methylisothiosemicarbazide can be explained with the absence of keto-imine form in the tautomeric equilibrium, which would allow the formation of a carbanion for further cyclization. This fact confirms the crucial role of the keto-imine tautomer A in the formation of AAMP.

## 4. Experimental section

### 4.1. General methods

IR spectrum was recorded on a Perkin–Elmer Spectrum One FT-IR spectrometer with a KBr disc. $^1$H and $^{13}$C NMR spectra were obtained using a Varian Gemini 200 spectrometer. Melting point was determined on a Mel-Temp capillary melting points apparatus, model 1001.

### 4.2. Procedure for the preparation of HDMCPI

*4.2.1. 5-Hydroxy-3,5-dimethyl-1-S-methylisothiocarbamoyl-2-pyrazolinium iodide (HDMCPI).* A mixture of thiosemicarbazide (9.10 g, 100 mmol) and methyl iodide (15.05 g, 106 mmol) in absolute ethanol (40 mL) was refluxed for 45 min. After 12 h, the separated white crystals of *S*-methylisothiosemicarbazide hydrogen iodide were filtered, washed with ethanol and used in the next step without further purification. Yield: 15.1 g (65%). A mixture of *S*-methylisothiosemicarbazide hydrogen iodide (11.65 g, 50 mmol) and acetylacetone (19.50 g, 195 mmol) in absolute ethanol (20 mL) was refluxed for 5 min. After cooling to room temperature, the crystallization was induced by rubbing the walls of the vessel with a glass stick. The light yellow crystals were filtered, washed three times with 5 mL of ether, and dried in air. Yield: 10.0 g (63%). Mp 157 °C. The suitable single crystals of HDMCPI for X-ray analysis were obtained by recrystallization from ethanol.

*4.2.1.1. Spectral data for HDMCPI.* IR (KBr, cm$^{-1}$): 3331, 3266, 3191, 3161, 3132, 2980, 1635, 1629, 1557, 1427, 1372, 1328, 1254, 1113, 733; $^1$H NMR (200 MHz, DMSO-$d_6$): $\delta$ 1.68 (3H, s, C$H_3$–C–OH), 2.04 (3H, s, C$H_3$–C=N), 2.55 and 2.62 (3H, two s, C$H_3$–S), $\delta_A$=3.24 and $\delta_B$=3.14 (2H, AB system, $J_{AB}$ 19.7 Hz, C$H_2$), 7.52 and 7.73 (1H, two br s, O*H*), 8.80, 8.96, and 9.42 (2H, three br s, nitrogen protons); $^{13}$C NMR (DMSO-$d_6$): $\delta$ 14.4 (*C*H$_3$–S), 16.7 (*C*H$_3$–C=N), 24.7 (*C*H$_3$–C–OH), 52.8 (C-4), 96.2 (C-5), 164.9 (NH$_2$–*C*(N)–S), 165.3 (C-3).

*4.2.1.2. NMR data for HDMCPI in $D_2O$.* $^1$H NMR (200 MHz, $D_2O$): $\delta$ 1.83 (3H, s, C$H_3$–C–OH), 2.13 (3H, s, C$H_3$–C=N), 2.65 (3H, s, C$H_3$–S), 3.32 (2H, s, C$H_2$); $^{13}$C NMR ($D_2O$): $\delta$ 16.3 (*C*H$_3$–S), 18.5 (*C*H$_3$–C=N), 26.8 (*C*H$_3$–C–OH), 55.2 (C-4), 98.9 (C-5), 168.5 (NH$_2$–*C*(N)–S), 168.7 (C-3).

*4.2.1.3. NMR data for HDMCPI at pD=9.5 (tautomeric form A).* $^1$H NMR (200 MHz, NaOD/$D_2O$): $\delta$ 1.95 and 2.07 (3H, two s, C$H_3$–C=N), 2.17 and 2.30 (3H, two s, C$H_3$–CO), 2.38 and 2.44 (3H, two s, C$H_3$–S); $^{13}$C NMR (NaOD/$D_2O$): $\delta$ 15.2 and 15.4 (*C*H$_3$–S), 19.9 and 24.8 (*C*H$_3$–C=N), 31.2 and 32.6 (*C*H$_3$–CO), 50.1 (complex signal, *C*H$_2$), 163.4 (CH$_3$–*C*=N), 163.8 (NH$_2$–*C*(N)–S), 214.3 (*C*O).

### 4.3. X-ray data collection and structure refinement

A light yellow prism shape single crystal of the compound 5-hydroxy-3,5-dimethyl-1-*S*-methylisothiocarbamoyl-2-pyrazolinium iodide (HDMCPI) was selected and mounted on glass fiber. Diffraction data were collected on an OXFORD DIFFRACTION KM4 four-circle goniometer equipped with SAPPHIRE CCD detector using graphite monochromated Mo K$\alpha$ X-radiation ($\lambda$=0.71073 Å) at 293 (2) K in the range 3.45 $\leq\theta\leq$26.37°. The crystals to detector distances were 45.0 mm. Crystal data: $C_7H_{14}IN_3OS$, Fwt.: 315.17, size: 0.69×0.37×0.23 mm, monoclinic, space group $P2_1/n$, $a$=12.204 (5) Å $b$=6.417(5) Å, $c$=15.995(5) Å, $\beta$=110.402(5)°, $V$=1174(1) Å$^3$, $T$=293(2) K, $Z$=4, $F$(000)=616, $D_x$=1.783 Mg m$^{-3}$, $\mu$=2.876 mm$^{-1}$. Cell parameters were determined by least-squares of the setting angles of 5004 (3.05$\leq\theta\leq$29.1°) reflections. A total of 4625 reflections were collected of which 2366 were unique [$R$(int)=0.0118, $R(\sigma)$=0.0183]; 1998 reflections were $>2\sigma$ ($I$). Completeness to $2\theta$=0.989. The data were reduced using the Oxford Diffraction program CrysAlis$^{pro}$.[22] A semiempirical absorption-correction based upon the intensities of equivalent reflections was applied (the minimum and maximum transmission factors were 0.53295 and 1.000), and the data were corrected for Lorentz, polarization, and background effects. Neutral atomic scattering factors, together with anomalous-dispersion corrections, were taken from the International Tables for X-ray Crystallography.[23] The structures were solved by direct methods (SIR-92) using program package WinGX,[24] and the figures were drawn using ORTEP[25] and MERCURY.[14] Anisotropic full-matrix least-squares refinement (SHEXL-97)[26] on $F^2$ for all non-hydrogen atoms yielded $R$1=0.0199 and $wR$2=0.0447 for 1998 [$I>2\sigma(I)$] and $R$1=0.0275 and $wR$2=0.0464 for all (2366) intensity data (goodness-of-fit=1.064; the maximum and mean shift/esd 0.002 and 0.000). Number of parameters=122. The maximum and minimum residual electron density in the final difference map was 0.302 and −0.385 e Å$^{-3}$. All hydrogen atomic positions could be located in the difference maps. The final refinement included atomic positional and displacement parameters for all non-H atoms. The isotropic displacement parameters of the hydrogen atoms were approximated from the $U$(eq) value of the atom they were bonded. The weighting schemes applied was $w$=1/[$\sigma^2(F_o^2)$+(0.0247$P$)$^2$+0.00648$P$] in **3**, where $P$=($F_o^2$+2$F_c^2$)/3.

Crystallographic data (excluding structure factors) have been deposited with the Cambridge Crystallographic Data Centre as supplementary publication number CCDC 755236. Copies of this information may be obtained free of charge from The Director, CCDC, 12 Union Road, Cambridge, CB2 1EZ, UK (fax: +44 1223 336033; e-mail: deposit@ccdc.cam.ac.uk or www: http://www.ccdc.cam.ac.uk).

### 4.4. Computational methods

All calculations were carried out using the Gaussian 03 program[27] using the B3LYP functional.[28–30] The 6-311++G(d,p) basis set was used for C, O, N, S, and H, whereas 6-311G(d,p) was employed for I. The geometrical parameters of all stationary points and transition states were optimized in water ($\epsilon$=78.36), using the conductor-like solvation model (CPCM).[31,32] All calculated structures were confirmed to be local minima (all positive eigenvalues) for ground state structures, or first-order saddle points (one negative eigenvalue) for transition state structures, by frequency calculations. The intrinsic reaction coordinates (IRCs), from the transition states down to the two lower energy structures, were traced using the IRC routine in Gaussian in order to verify that each saddle point is linked with two putative minima. The results of the IRC calculations for two crucial transition states, TS4 and TS6, are presented in Figs S2 and S3 of Supplementary data. Evolution of

relevant bonds along the reaction pathway was estimated using the natural bond orbital analysis.[33]

## Acknowledgements

The work was financed by the Ministry for Science of the Republic of Serbia (Grants N$^{o}$ 142028 and 142025) and the Provincial Secretariat for Science and Technological Development of Vojvodina.

## Supplementary data

Electronic supplementary data available: X-ray crystallographic and computational data. Supplementary data associated with this article can be found, in the online version, at doi:10.1016/j.tet.2010.05.093. These data include MOL files and InChIKeys of the most important compounds described in this article.

## References and notes

1. Pevarello, P.; Brasca, M. G.; Amici, R.; Orsini, P.; Traquandi, G.; Corti, L.; Piutti, C.; Sansonna, P.; Villa, M.; Pierce, B. S.; Pulici, M.; Giordano, P.; Martina, K.; Fritzen, E. L.; Nugent, R. A.; Casale, E.; Cameron, A.; Ciomei, M.; Roletto, F.; Isacchi, A.; Fogliatto, G.; Pesenti, E.; Pastori, W.; Marsiglio, A.; Leach, K. L.; Clare, P. M.; Fiorentini, F.; Varasi, M.; Vulpetti, A.; Warpehoski, M. A. *J. Med. Chem.* **2004**, *47*, 3367–3380.
2. Pevarello, P.; Brasca, M. G.; Orsini, P.; Traquandi, G.; Longo, A.; Nesi, M.; Orzi, F.; Piutti, C.; Sansonna, P.; Varasi, M.; Cameron, A.; Vulpetti, A.; Roletto, F.; Alzani, R.; Ciomei, M.; Albanese, C.; Pastori, W.; Marsiglio, A.; Pesenti, E.; Fiorentini, F.; Bischoff, J. R.; Mercurio, C. *J. Med. Chem.* **2005**, *48*, 2944–2956.
3. Samanta, S.; Debnath, B.; Basu, A.; Gayen, S.; Srikanth, K.; Jha, T. *Eur. J. Med. Chem.* **2006**, *41*, 1190–1195.
4. Pevarello, P.; Fancelli, D.; Vulpetti, A.; Amici, R.; Brasca, M. G.; Amici, R.; Villa, M.; Pittala, V.; Vianello, P.; Cameron, A.; Ciomei, M.; Mercurio, C.; Bischoff, J. R.; Roletto, F.; Varasi, M.; Brasca, M. G. *Bioorg. Med. Chem. Lett.* **2006**, *16*, 1084–1090.
5. Shapiro, G. I. *J. Clin. Oncol.* **2006**, *24*, 1770–1783.
6. Misra, R. N. *Drugs Future* **2006**, *31*, 43–52.
7. Castoldi, R. E.; Pennella, G.; Saturno, G. S.; Grossi, P.; Brughera, M.; Venturi, M. *Curr. Opin. Drug Discovery Dev.* **2007**, *10*, 53–57.
8. Carpinelli, P.; Ceruti, R.; Giorgini, M. L.; Cappella, P.; Gianellini, L.; Croci, V.; Degrassi, A.; Texido, G.; Rocchetti, M.; Vianello, P.; Rusconi, L.; Storici, P.; Zugnoni, P.; Arrigoni, C.; Soncini, C.; Alli, C.; Patton, V.; Marsiglio, A.; Ballinari, D.; Pesenti, E.; Fancelli, D.; Moll, J. *Mol. Cancer Ther.* **2007**, *6*, 3158–3168.
9. Bebbington, D.; Binch, H.; Charrier, J. D.; Everitt, S.; Fraysse, D.; Golec, J.; Kay, D.; Knegtel, R.; Mak, C.; Mazzei, F.; Miller, A.; Mortimore, M.; O'Donnell, M.; Patel, S.; Pierard, F.; Pinder, J.; Pollard, J.; Ramaya, S.; Robinson, D.; Rutherford, A.; Studley, J.; Westcott, J. *Bioorg. Med. Chem. Lett.* **2009**, *19*, 3586–3592.
10. Velcicky, J.; Feifel, R.; Hawtin, S.; Heng, R.; Huppertz, C.; Koch, G.; Kroemer, M.; Moebitz, H.; Revesz, L.; Scheufler, C.; Schlapbach, A. *Bioorg. Med. Chem. Lett.* **2009**, , doi:10.1016/j.bmcl.2009.10.138
11. Hergold-Brundić, A.; Kaitner, B.; Kamenar, B.; Leovac, V. M.; Ivegeš, E. Z.; Juranić, N. *Inorg. Chim. Acta* **1991**, *188*, 151–158.
12. Grell, J.; Bernstein, J.; Tinhofer, G. *Acta Cryst., Sect. B* **2000**, *56*, 166.
13. Spek, A. L. *J. Appl. Crystallogr.* **2003**, *36*, 7–13.
14. Macrae, C. F.; Edgington, P. R.; McCabe, P.; Pidcock, E.; Shields, G. P.; Taylor, R.; Towler, M. v. d.; Streek, J. *J. Appl. Crystallogr.* **2006**, *39*, 453–457.
15. Zelenin, K. N.; Alekseev, V. V.; Zelenin, A. K.; SushkovaYu, S. *Chem. Heterocycl. Compd.* **1999**, *35*, 87–92.
16. Casas, J. S.; Castano, M. V.; Castellano, E. E.; Ellena, J.; García-Tasende, M. S.; Gato, A.; Sánchez, A.; Sanjuán, L. M.; Sordo, J. *Inorg. Chem.* **2002**, *41*, 1550–1557.
17. Zelenin, K. N.; Alekseyev, V. V. *Top. Heterocycl. Syst.* **1996**, *1*, 141–156.
18. Katritzky, A. R.; Ghiviriga, I.; Oniciu, D. C.; O'Ferrall, R. A. M.; Walsh, S. M. *J. Chem. Soc., Perkin Trans. 2* **1997**, 2605–2608.
19. Yamazaki, C. *Can. J. Chem.* **1975**, *53*, 610–615.
20. Szabó, A.; Cesljevic, V. I.; Kovács, A. *Chem. Phys.* **2001**, *270*, 67–78.
21. Zelenin, K. N.; Potapov, A. A.; Alekseyev, V. V.; Lagoda, I. V. *Chem. Het. Comp.* **2004**, *40*, 903–910.
22. Data collection and processing software, Vers.1 2006, (Oxford Diffraction Ltd, 68 Milton Park, OX144RX, UK).
23. *International Tables for X-ray Crystallography*; Wilson, A. J. C., Ed.; Kluwer Academic: Dordrecht, 1992; Vol C, pp 500–502; 219–222, 193–199.
24. Farrugia, L. J. *J. Appl. Crystallogr.* **1999**, *32*, 837–838.
25. Farrugia, L. J. *J. Appl. Crystallogr.* **1997**, *30*, 565.
26. Sheldrick, G. M. *SHELXL-97 Program for the Refinement of Crystal Structures*; University of Göttingen: Göttingen, 1997.
27. Frisch, M. J.; Trucks, G. W.; Schlegel, H. B.; Scuseria, G. E.; Robb, M. A.; Cheeseman, J. R.; Montgomery, J. A., Jr.; Vreven, T.; Kudin, K. N.; Burant, J. C.; Millam, J. M.; Iyengar, S. S.; Tomasi, J.; Barone, V.; Mennucci, B.; Cossi, M.; Scalmani, G.; Rega, N.; Petersson, G. A.; Nakatsuji, H.; Hada, M.; Ehara, M.; Toyota, K.; Fukuda, R.; Hasegawa, J.; Ishida, M.; Nakajima, T.; Honda, Y.; Kitao, O.; Nakai, H.; Klene, M.; Li, X.; Knox, J. E.; Hratchian, H. P.; Cross, J. B.; Adamo, C.; Jaramillo, J.; Gomperts, R.; Stratmann, R. E.; Yazyev, O.; Austin, A. J.; Cammi, R.; Pomelli, C.; Ochterski, J. W.; Ayala, P. Y.; Morokuma, K.; Voth, G. A.; Salvador, P.; Dannenberg, J. J.; Zakrzewski, V. G.; Dapprich, S.; Daniels, A. D.; Strain, M. C.; Farkas, O.; Malick, D. K.; Rabuck, A. D.; Raghavachari, K.; Foresman, J. B.; Ortiz, J. V.; Cui, Q.; Baboul, A. G.; Clifford, S.; Cioslowski, J.; Stefanov, B. B.; Liu, G.; Liashenko, A.; Piskorz, P.; Komaromi, I.; Martin, R. L.; Fox, D. J.; Keith, T.; Al-Laham, M. A.; Peng, C. Y.; Nanayakkara, A.; Challacombe, M.; Gill, P. M. W.; Johnson, B.; Chen, W.; Wong, M. W.; Gonzalez, C.; Pople, J. A. *Gaussian 03, E.01-SMP*; Gaussian: Pittsburgh, PA, 2003.
28. Becke, A. D. *Phys. Rev. A.* **1988**, *38*, 3098–3100.
29. Lee, C.; Yang, W.; Parr, R. G. *Phys. Rev. B* **1988**, *37*, 785–789.
30. Becke, A. D. *J. Chem. Phys.* **1993**, *98*, 5648–5652.
31. Barone, V.; Cossi, M. *J. Phys. Chem. A* **1998**, *102*, 1995–2001.
32. Cossi, M.; Rega, N.; Scalmani, G.; Barone, V. *J. Comput. Chem.* **2003**, *24*, 669–681.
33. Foster, J. P.; Weinhold, F. *J. Am. Chem. Soc.* **1980**, *102*, 7211–7218.